

# Piezoelectric and dielectric reliability of lead zirconate titanate thin films

Ronald G. Polcawich and Susan Trolier-McKinstry  
*The Pennsylvania State University, Materials Research Laboratory,  
University Park, Pennsylvania 16802*

(Received 12 October 1999; accepted 16 August 2000)

This work was directed toward developing a database for the long-term reliability of the transverse piezoelectric coefficient  $d_{31}$  under both unipolar and bipolar drive. Under unipolar drive, the films showed excellent reliability, with 99% of the devices surviving to  $10^9$  cycles. However, both aging and low amplitude bipolar drive resulted in rapid degradation of  $d_{31}$  due to backswitching of the ferroelectric domains. Both thermal and ultraviolet (UV) imprint prevented backswitching and resulted in improved aging and bipolar degradation behavior. Additionally, the UV imprinted samples showed nonlinear aging due to the presence of an internal space charge field that developed from photo-induced charge carriers.

## I. INTRODUCTION

There is significant interest in lead zirconate titanate (PZT) thin films for sensors, actuators, and microelectromechanical systems (MEMS). With piezoelectric coefficients an order of magnitude larger than aluminum nitride (AlN) and zinc oxide (ZnO),<sup>1,2</sup> PZT films can provide low voltage, high amplitude actuation. One of the key questions for device development is the reliability of PZT-based microdevices. To date, however, only a few electromechanical reliability studies have been reported.

A majority of the available literature to date has focused on determining the aging and large alternating current (ac) electric field reliability of the longitudinal piezoelectric coefficient  $d_{33}$ .<sup>3,4</sup> The results during unipolar drive are the most promising, with little degradation witnessed in the piezoelectric response out to  $10^9$  cycles. Unfortunately, aging and bipolar degradation result in substantial losses in the longitudinal piezoelectric coefficient over time. Separate studies on both  $d_{33}$  and  $d_{31}$  have concluded that "spontaneous depoling" is the cause of the rapid aging of the piezoelectric coefficients.<sup>3,5,6</sup>

While the work on the longitudinal piezoelectric coefficient is illustrative, a majority of MEMS device structures require the transverse piezoelectric coefficient  $d_{31}$  for sensing and actuation. Consequently, this work focused on studying the factors that affect the stability of the  $d_{31}$  coefficient.

Using the wafer flexure technique<sup>7</sup> to evaluate the transverse piezoelectric response, an analysis of aging, high field unipolar, and small amplitude bipolar drive reliability was performed to assess the lifetime of PZT thin-film devices. This work was designated to determine the piezoelectric reliability of PZT thin films under vari-

ous electrical stresses and determine the specific mechanism(s) contributing to electromechanical degradation.

To improve upon piezoelectric reliability, a mechanism to prevent depoling in PZT thin films is necessary. Creating a preferred polarization state within the ferroelectric is known to be effective in preventing depoling in bulk ceramics, and is widely utilized in hard PZT compositions for actuator applications. A preferred polarization state may be achieved by stabilizing a particular domain orientation.

The idea of locking in a domain configuration is formally known as imprint and has been extensively studied as a factor limiting reliability in ferroelectric memories (where repetitive switching is required).<sup>8-10</sup> There are two main methods of achieving imprint. First, poling PZT films while illuminating them with ultraviolet radiation has been shown to shift the polarization electric field (P-E) hysteresis loop along the field axis through the alteration of the spatial location of the internal space charges.<sup>8</sup> The second imprint method utilizes thermal energy to align defect dipole complexes ( $V_{Pb}'' - V_O^{\bullet\bullet}$ ,  $Fe_{Ti}' - V_O^{\bullet\bullet}$ , etc.) to create an internal electric field aligned with the polarization direction.<sup>11</sup> The final section of this work focused on ultraviolet illumination and thermal imprint techniques as a means of improving the piezoelectric reliability by stabilizing a domain configuration such that depoling is minimized.

## II. EXPERIMENTAL PROCEDURE

### A. Preparation of PZT thin films

PZT thin films with a Zr/Ti ratio of 52/48 were synthesized using a modification of the procedure described by Budd et al.<sup>12</sup> using lead acetate trihydrate, titanium-

IV isopropoxide, and zirconium-IV propoxide as precursors and 2-methoxyethanol as a solvent (Aldrich Chemical, Milwaukee, WI). Additionally, 4 vol% formamide (Aldrich Chemical) was added as a drying control agent after refluxing. The resultant PZT solution had a concentration of 0.4 M.

Platinized (100) silicon wafers (Nova Electronics, Richardson, TX), 7.6 cm in diameter, were used as substrates. The wafer surface was coated with a 1- $\mu\text{m}$  thermal oxide, a sputtered 200- $\text{\AA}$  titanium buffer layer, and a 1500- $\text{\AA}$  sputtered platinum layer. The substrates were first blown clean with ultra-high-purity nitrogen and dried on a hotplate at 340  $^{\circ}\text{C}$  for 1 min. A syringe with a 0.1- $\mu\text{m}$  Whitman filter (Aldrich Chemical) was used to deposit solution onto the stationary substrate prior to spinning for 30 s at 3000 rpm. Next, the film was pyrolyzed on a hotplate at 340  $^{\circ}\text{C}$  for 1 min. Crystallization occurred after the deposition and pyrolysis process was repeated 4 times. A Heatpulse 610 rapid thermal annealing furnace (A.G. Associates, San Jose, CA) was used to complete crystallization using a dwell at 700  $^{\circ}\text{C}$  for 30 s. Deposition, pyrolysis, and crystallization continued until a final film thickness of approximately 1.0  $\mu\text{m}$  was achieved. Typical ferroelectric, dielectric, and piezoelectric properties of the films are reported in Table I.

## B. Electrical contacts

Glow discharge sputtering through a 1.5-mm-diameter shadow mask was used to deposit platinum electrodes on the PZT thin films. A postanneal at 385–400  $^{\circ}\text{C}$  for 60 s was performed to remove sputtering-induced surface damage or contamination at the film–electrode interface. Two methods were utilized to make contact to the capacitors. One method involved using micro positioners (Signatone, Gilroy, CA) with fine tungsten tips to make a pressure contact with the platinum. Alternatively, a 2-cm-long steel wire was attached perpendicular to the film surface near the top electrode with Circuit Works conductive epoxy (Chemtronics Inc., Kennesaw, GA). The epoxy contacted a small section of the Pt electrode with the steel wire used as a connection post to solder an electrical lead from the instrumentation. The measured dielectric properties of the films did not depend on the contact method.

TABLE I. Ferroelectric, dielectric, and piezoelectric properties of approximately 1.0- $\mu\text{m}$  PZT thin films.

Remanent Polarization, $P_r$	20–25 $\mu\text{C}/\text{cm}^2$
Coercive Field, $E_c$	38–42 $\text{kV}/\text{cm}$
$\epsilon_{33}$	1000–1100
$\tan \delta$	2–4%
$d_{31}$	–25 to –40 $\text{pC}/\text{N}$

## C. High and low field ferroelectric and dielectric characterization

Using a RT66A ferroelectric tester (Radiant Technologies, Albuquerque, NM) the remanent polarization  $P_r$  and the coercive field  $E_c$  were measured. The maximum applied voltage ranged from 15 to 20 V depending on film thickness. Low field measurements of the dielectric constant and dielectric loss were performed using a 4192A LF impedance analyzer (Hewlett-Packard, Palo Alto, CA) at a frequency of 10 kHz with a peak-to-peak voltage of 30 mV.

## D. Measurement of the transverse piezoelectric coefficient

The wafer flexure technique<sup>7</sup> was used to measure the transverse ( $d_{31}$ ) piezoelectric coefficient. This technique uses the oscillation of a 10-in. audio speaker to generate periodic changes of air pressure in an aluminum air cavity housed beneath a PZT-coated Si wafer. These oscillations periodically flex the wafer, applying a biaxial stress to the wafer and PZT film. Using the direct piezoelectric response, the film  $d_{31}$  is calculated via

$$d_{31} = \frac{Q}{AX_{\text{film}}}, \quad (1)$$

where  $Q$  is the surface charge,  $A$  is the electrode area, and  $X_{\text{film}}$  is the biaxial stress on the PZT thin film. A Young's modulus of 101 GPa<sup>13</sup> was used for the PZT film, along with the elastic properties of the Si substrate and small deflection plate theory to calculate  $X_{\text{film}}$  on the basis of the known pressure difference between the cavity and the ambient. Experiments throughout this work used a poling procedure with the top electrode being positively biased, resulting in polarization directed toward the bottom electrode.

## E. Reliability of PZT film under ac electric field drive

Unipolar and bipolar ac electrical fields at frequencies ranging from 1 to 100 kHz were applied to determine the reliability of PZT thin films. The changes in the piezoelectric, ferroelectric, and dielectric properties were monitored over time by intermittently removing the applied electric field. Values of the unipolar electric field ranged from 120 to 400  $\text{kV}/\text{cm}$ , while that of the bipolar field ranged from 10 to 30  $\text{kV}/\text{cm}$ . Experiments were initiated by poling the film for 15 min, aging for 5 min, measuring baseline values for  $d_{31}$ ,  $\epsilon_{33}$ , and  $\tan \delta$ , applying the electric field, and intermittently measuring the piezoelectric and dielectric properties.

## F. Imprint of PZT films

Two procedures were followed to generate imprint in PZT thin films. In the first, samples were poled while illuminating with an ultraviolet (UV) radiation source. A

365-nm Hg source lamp (UVP Inc., Upland, CA) was used to illuminate 25–50 mW/cm<sup>2</sup> onto the PZT thin film. To achieve penetration through the top electrode, semitransparent (approximately 150 Å thick) Pt electrodes were deposited. Second, poling at 150 °C was used as a means to generate imprint by aligning defect dipoles. Poling times varied from 10 to 20 min at electric fields of 200–240 kV/cm.

### III. RESULTS AND DISCUSSION

#### A. Aging

The PZT films used in this work had aging rates at room temperature and under dark conditions of 6–12% per decade for  $d_{31}$  and 1–3% per decade for  $\epsilon_{33}$  (see Fig. 1), which agreed well with values reported in the literature.<sup>3,5</sup> The presence of such a large difference in the aging rates of these two properties suggests that different mechanisms are responsible for the aging behavior of each parameter.<sup>3</sup> The decay in the dielectric properties has been attributed to domain wall pinning in both bulk and thin film ceramics.<sup>3,14</sup> On the other hand, the rapid decline in the piezoelectric response of thin films is believed to be the result of loss of polarization due to back-switching of the ferroelectric domains.<sup>3,5,6</sup>

#### B. Effect of a unipolar ac electric field

To achieve large strains in a piezoelectric material, a large electric field must be applied. To assess the reliability of the transverse piezoelectric response under large electric fields, unipolar square pulsed ac electric fields were applied to PZT piezoelectric capacitors. The results presented in Fig. 2 show that devices can survive

to 10<sup>9</sup> unipolar cycles with no decrease in the piezoelectric response for electric field amplitudes from 3 to 5  $E_c$  (approximately 120–200 kV/cm). The increase in the magnitude of  $d_{31}$  is a result of improved poling of the PZT capacitors.

The observed behavior of the piezoelectric response agreed with results presented by Wang *et al.*<sup>15</sup> and Kholkin *et al.*<sup>4</sup> on PZT ceramics and thin films, respectively. For thin films, the increase in  $d_{33}$  was explained as the gradual build up of an internal field during cycling. This was evidenced by examining polarization electric field hysteresis loops after the capacitors completed various numbers of cycles. The end result, as seen in Fig. 3, was a shift of the piezoelectric electric field hysteresis

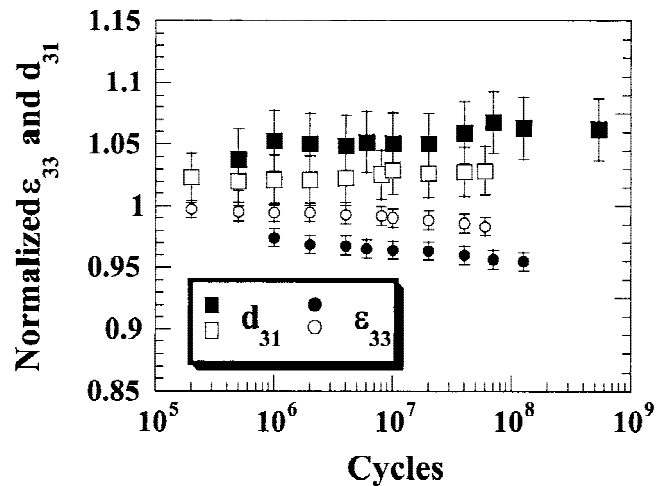


FIG. 2. Characteristic changes in the  $d_{31}$  and  $\epsilon_{33}$  coefficient during unipolar cycling with a maximum electric field of 3 and 5  $E_c$  (approximately 120–200 kV/cm). Error bars illustrate the range of values obtained in several experiments.

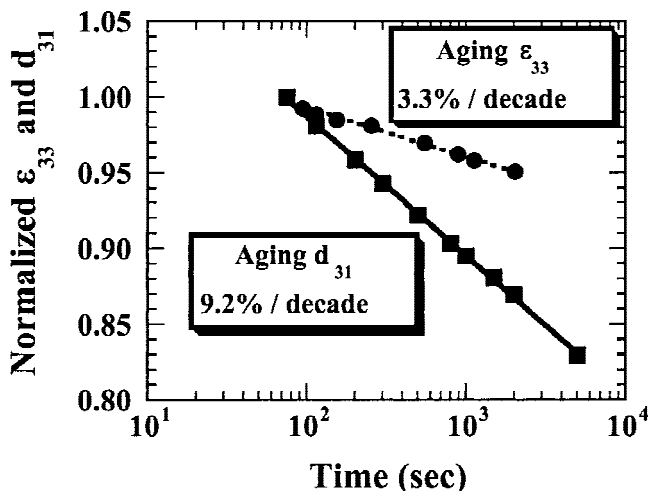


FIG. 1. Aging of the dielectric permittivity  $\epsilon_{33}$  and the transverse piezoelectric coefficient  $d_{31}$ . Aging rates for  $\epsilon_{33}$  of 1–3% per decade are typical, while the  $d_{31}$  coefficient ages at rates of 6–12% per decade.

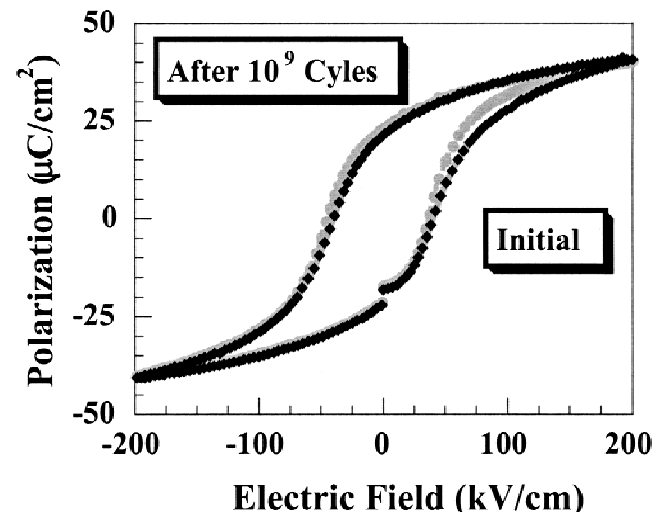


FIG. 3. Shift in the polarization electric field hysteresis loop after unipolar drive at 200 kV/cm. The magnitude of the shift is 4.9 kV/cm.

loop along the field axis. The P-E loop shifted 4–6 kV/cm along the field axis and increased the negative field required to switch the polarization from the positive remanent state. It is believed, given the low mobility of non-180° domain walls in PZT films under a micron in thickness,<sup>5,16,17</sup> that the internal field is more important than changes in the extrinsic contribution (i.e., non-180° domain wall motion) to  $d_{31}$  in controlling the behavior during cycling.

A second aspect of Fig. 2 is the steady decline of  $\epsilon_{33}$  during unipolar drive. The dielectric constant comprises both an intrinsic contribution (associated with the appropriate averaging of the single-domain, single-crystal response to the applied field) and an extrinsic contribution due primarily to domain wall motion.<sup>18</sup> Thus, one possibility for the observed decline in the dielectric constant is a decrease in the extrinsic contribution to the dielectric constant by the pinning or elimination of 180° domain walls. Alternatively, it is possible that the internal electric field developed during ac cycling could also account for the permittivity decrease.

### C. Bipolar ac electric field drive

If domain backswitching contributes to the rapid piezoelectric aging behavior, then cycling with a small amplitude bipolar ac field should result in even faster degradation rates. Due to the nonsquare nature of the P-E hysteresis response, a film poled at positive remanence will subsequently lose a degree of its polarization with the application of a negative electric field. Therefore, the larger the magnitude of a bipolar ac electric field, the greater the degree of polarization reversal. Figure 4 confirms the amplitude dependence and suggests that field-

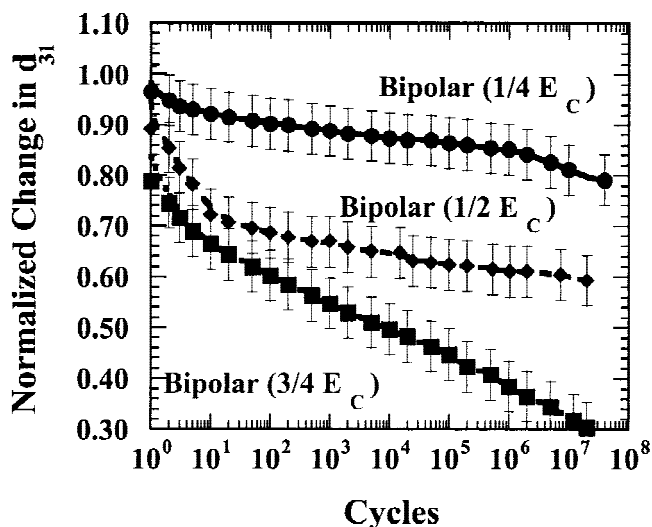


FIG. 4. Amplitude dependence of bipolar degradation with each curve representing the typical behavior observed at a specified cycling field. The ranges given are indicative of sample-to-sample variability.

induced depoling does, in fact, contribute to the rapid electromechanical degradation during bipolar drive. After poling most domains are aligned with the applied field, however a portion of the domains may contain local electric fields which oppose the remanent polarization. For these domains, the application of a field antiparallel to the poling field provides the necessary energy to backswitch to a more stable domain configuration. As witnessed, field-induced depoling has a very dramatic effect on piezoelectric reliability.

To check whether or not the field-induced depoling was associated with a temperature rise associated with the driving, the temperature of a sample was monitored during cycling with a 30 gauge thermocouple wire placed on the film within approximately 1 mm of the measured top electrode and held in place with tape. It is assumed that the temperature is uniform in the vicinity of the driven sample due primarily to the large thermal conductivity of the underlying silicon substrate. A temperature change of about 2–5 °C was noted during cycling. This small temperature change will not cause a substantial degree of depoling. Therefore, field-induced depoling is the most likely mechanism causing the decline in  $d_{31}$  during cycling.

### D. Effect of imprint on aging

Using the two imprint techniques described previously, dramatic improvements in the aging behavior occurred. Each of the imprint techniques shifted the polarization electric field approximately 20–25 kV/cm along the voltage axis. Figure 5 presents the results of the various imprint procedures on the aging behavior. Thermal poling led to the greatest improvement, with initially larger  $d_{31}$  values and reduced aging rates of 2–3%/decade. Thermal imprint increased the magnitude of  $d_{31}$  by  $36\% \pm 11\%$  due to improved poling. Similar increases in the  $d_{33}$  piezoelectric response have been obtained on PZT thin films.<sup>19</sup> The thermal energy facilitates alignment of a greater percentage of domains with the poling field. The simultaneous alignment of defect dipoles with the applied electric field (as previously confirmed with electron paramagnetic resonance measurements),<sup>11</sup> creates an internal electric field shifting the P-E loop on the field axis, and decreases the likelihood of progressive backswitching. Thus, in addition to larger piezoelectric coefficients, aging rates of  $d_{31}$  for thermally imprinted devices are significantly reduced.

Additionally, thermal poling reduces the magnitude of the dielectric constant (approximately 14%) and loss tangent (approximately 20%). When samples were cooled to 4 K, the permittivity difference between normally poled and thermally poled samples disappeared (see Fig. 6). In principle, the observed difference in the dielectric constant after imprint could be a result of the internal bias

field depressing the measured permittivity. However, were this the case, the field-induced difference in permittivity values before and after imprint should have been retained even near absolute zero. On the other hand, it is well known that since domain wall motion is thermally activated, extrinsic contributions to the permittivity are frozen out at low temperatures.<sup>20</sup> Thus the convergence of the dielectric constants of permittivity data with decreasing temperature is consistent with the supposition that the thermally poled sample shows less extrinsic contributions to the permittivity than do normally poled films. The convergence of the two curves at low temperatures also confirms that the decreased room-temperature permittivity after hot poling is not due to a large amount of non-180° domain reversal in the poling process (which would change the permittivities at all temperatures due to the anisotropy between  $\epsilon_{33}$  and  $\epsilon_{11}$  in PZT). Thus, the decreased  $\epsilon_{33}$  in thermally poled samples could be a result of either a reduction in the density of domain walls or a decrease in domain wall mobility.<sup>19</sup> The reduction in  $\tan \delta$  could be due to a combination of this decrease in domain wall contributions, a decrease in the concentration of trapped space charge, and more stable defect dipoles.

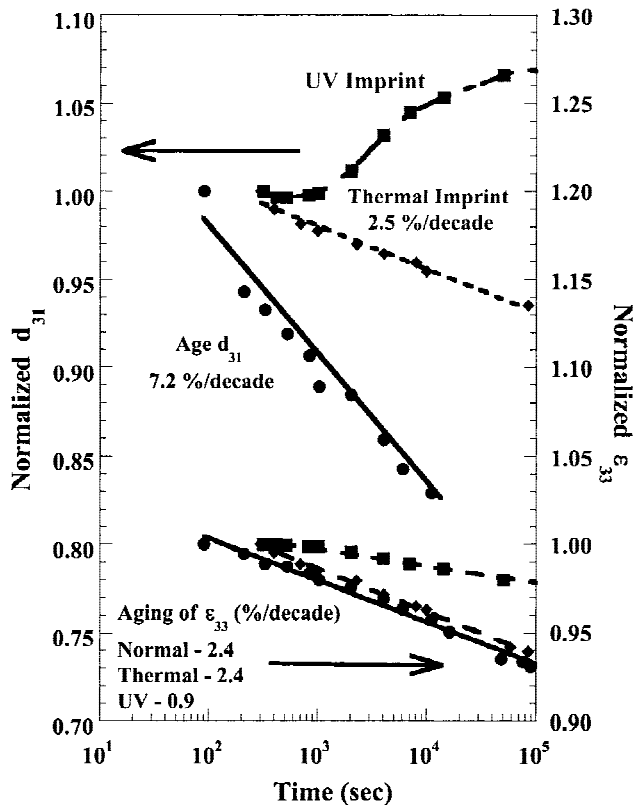


FIG. 5. Imprint effects on aging. Thermal imprint reduces the aging rate from 6 to 12%/decade to 2–3%/decade. UV imprint results in nonlinear aging with increases in  $d_{31}$  commencing approximately  $10^3$  seconds after poling.

Aging results for UV-imprinted devices are quite different from those of thermally imprinted devices. The dielectric constant is lowered by  $11\% \pm 3\%$  relative to normally poled samples. The lower values of the dielectric constant can be explained by a reduction in 180° domain wall concentration or mobility as photo-induced charge carriers are trapped at domain boundaries after UV exposure. Relative to normal poling, UV imprint sometimes led to increases and sometimes to decreases in the piezoelectric response of up to 10%, depending at least in part on whether the capacitors were previously exposed to UV illumination during earlier experiments on other electrodes. The increases in the piezoelectric response agreed with the results of Kholkin *et al.*<sup>21</sup> in which substantial increases in  $d_{33}$  occurred when films were subjected to UV illumination during poling. The origin of the decrease in  $d_{31}$  sometimes observed on UV

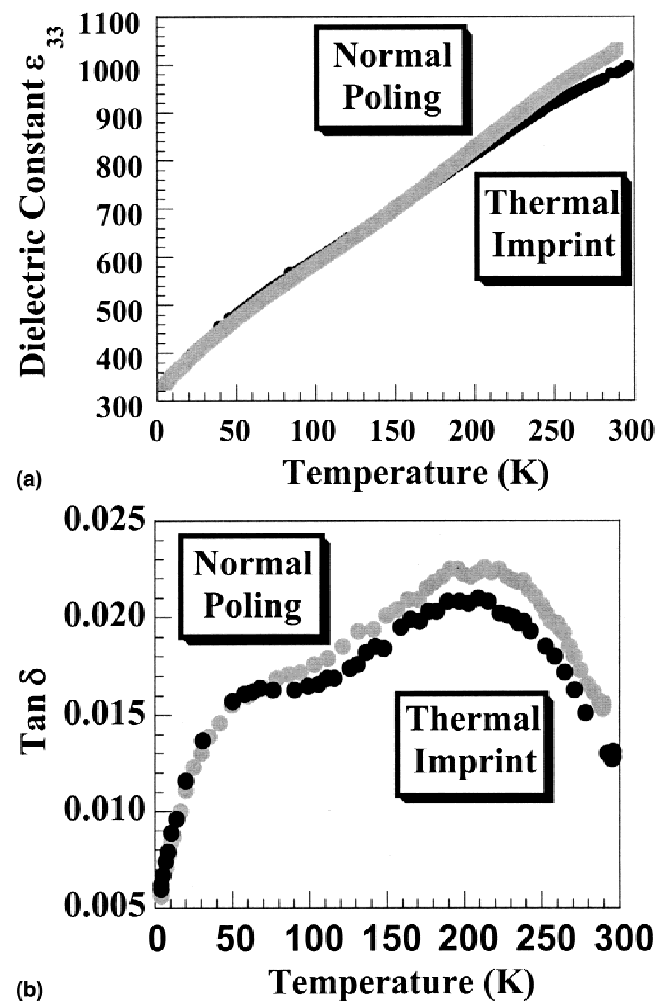


FIG. 6. Effect of thermal imprint on the temperature dependence of (a)  $\epsilon_{33}$  (b)  $\tan \delta$ . Differences in the room-temperature dielectric properties for thermally imprinted and normally poled films are eliminated at 4 K.

poling is not yet clear, but may result from the presence of excess charge carriers present in the piezoelectric from earlier experiments.

After UV poling, the subsequent aging behavior of  $\epsilon_{33}$  was normal, with reduced aging rates of approximately 0.9%/decade (see Fig. 5). However, the aging behavior of  $d_{31}$  is nonlinear (see Fig. 5). Apparently, near  $10^3$  seconds after poling and exposure, there is a gradual increase in the value of the piezoelectric coefficient. This rise continues until  $10^5$ – $10^6$  seconds where the d-coefficient remains nearly constant or begins to decline.

To ascertain the mechanism(s) responsible for the aging behavior of the piezoelectric response in UV-imprinted films; samples were normally poled, aged, subsequently illuminated with UV radiation, and further aged. The goal was to determine whether a space charge field associated with photo-induced charges was responsible for the observed behavior in the transverse piezoelectric coefficient. The results from the experiments are presented in Fig. 7 with schematic diagrams in Fig. 8 to illustrate potential mechanisms responsible for the behavior of  $d_{31}$  after illumination. Prior to illumination, the film ages at a usual rate of 7%/decade. Upon illumination, the value of the piezoelectric coefficient immediately drops and then continues to decrease with time. This sharp decrease in  $d_{31}$  with illumination is probably a result of depoling of unstable domains and/or back-switching due to the generated photovoltage. As electrons are excited from domain boundaries [see Fig. 8(b)], some domains may re-orient with the depolarization field as the free carriers reduce the electrostatic potential barrier for domain reorientation<sup>10</sup> [see Figure 8(c)]. The result is a reduced net polarization,  $P_{\text{net}}$  and subsequently a diminished transverse piezoelectric response. Additionally, a photovoltage develops due to the photovoltaic effect. Photo-generated charges migrate under the influence of the polarization potential.<sup>22</sup> The resulting buildup of free carriers generates a photovoltage across the sample.<sup>22</sup> This field is oriented anti-parallel with the direction of the polarization and can be large enough to result in some degree of domain back-switching.<sup>22</sup> The result is a decreased  $P_{\text{net}}$  and  $d_{31}$ .

Continued decreases in  $d_{31}$  during exposure may occur as charge carriers migrate due to the photovoltaic effect. Therefore, during illumination an internal field develops opposing the direction of polarization [see Figure 8(d)]. This field reduces the net charge available for measuring the transverse piezoelectric response. Thus,  $d_{31}$  diminishes during UV exposure as the magnitude of the internal field increases.

Another possibility is that an internal field arises from the Dember effect.<sup>23</sup> A concentration gradient of charge carriers develops from nonuniform illumination through the sample depth due to a progressive drop in light intensity associated with absorption in the film and the top electrode.<sup>21</sup> Consequently, the charge carriers migrate to eliminate this gradient [see Figure 8(e)]. The lower mobility of holes<sup>10</sup> reduces the diffusion distance compared to electrons, resulting in an internal electric field. This internal field will be directed toward the bottom elec-

trode.<sup>21</sup> Consequently, the charge carriers migrate to eliminate this gradient [see Figure 8(e)]. The lower mobility of holes<sup>10</sup> reduces the diffusion distance compared to electrons, resulting in an internal electric field. This internal field will be directed toward the bottom elec-

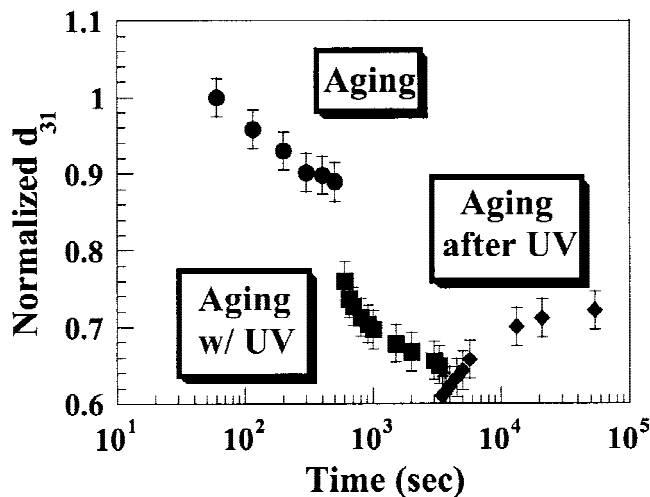


FIG. 7. Changes in the piezoelectric response in response to UV illumination. Prior to exposure, the device ages at 7%/decade. Upon illumination, there is a sharp decline in  $d_{31}$  in response to a depoling mechanism. Subsequent decreases are the result of the buildup of a space charge field. After illumination,  $d_{31}$  again drops but then begins to rise as the space charge field diminishes. Error bars are representative of the range of values observed among several similar experiments.

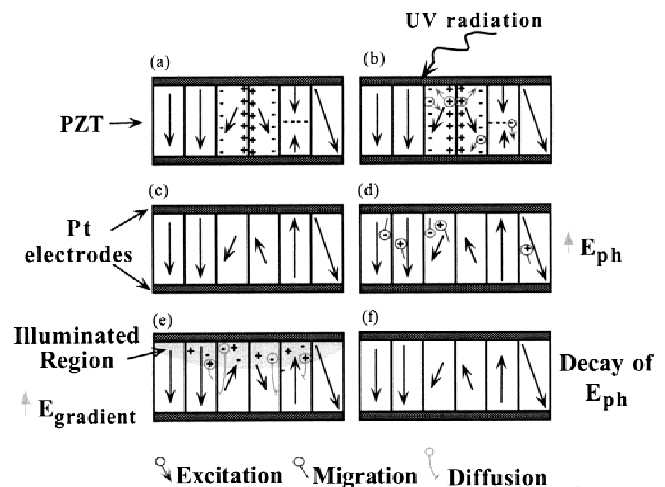


FIG. 8. Schematic diagrams illustrating possible mechanisms responsible for the aging behavior of UV-exposed samples: (a) initial normally poled sample with the applied field ( $E_{\text{app}}$ ) directed toward the bottom electrode, (b) photo-excitation of charge carriers by UV illumination, (c) metastable domains back-switch, aligning with depolarization field ( $E_{\text{dep}}$ ), (d) migration of photo-induced charge carriers, resulting in a photoelectric field ( $E_{\text{ph}}$ ), (e) development of an internal space charge field due to a charge carrier concentration gradient ( $E_{\text{gradient}}$ ), (f) decay of the internal field due to migration and recombination of excess charge carriers.

trode, resulting only in a net decrease in piezoelectric charge for films with a polarization directed toward the top electrode.

Behavior like that shown in Fig. 7 was observed with samples poled up and down. The independence of the aging behavior on poling direction eliminates a charge carrier concentration gradient as the controlling mechanism for the observed aging behavior. Thus, it is concluded that the continued decrease in  $d_{31}$  during illumination results from an increasing internal field associated with the photovoltaic effect. The presence of this field limits the charge generated by the direct piezoelectric response, resulting in a lower value for the measured piezoelectric coefficients.

Upon removal of the UV illumination, there is again a sharp decline in  $d_{31}$ . The reason for the decline is unclear but a possible explanation is a further increase in the space charge field as generation/recombination interactions diminish and charges are trapped. The subsequent aging after illumination is similar to that created by UV assisted poling (in which an increase in  $d_{31}$  commences approximately  $10^3$  seconds after illumination). This rise in  $d_{31}$  is believed to be associated with the decay of the internal space charge field as charge carriers recombine or migrate due to the finite dark conductivity [see Fig. 8(f)]. The annihilation or migration of charge carriers diminishes the space charge field. Subsequently, the net charge available for measurement in the piezoelectric response increases, resulting in an increased  $d_{31}$  coefficient.

### E. Effect of imprint on bipolar degradation

Imprint also improves the bipolar degradation behavior of PZT films, as shown in Fig. 9. Compared to normal poling, in which about 30% losses of the original  $d_{31}$  value were seen after  $10^9$  cycles, imprinted films retain at least 90% of their original  $d_{31}$  values after  $10^9$  bipolar cycles with a field of 20 kV/cm. Again, increases in  $d_{31}$  occur near  $10^3$  seconds for UV-imprinted films.

The dielectric constant of thermally imprinted samples showed the same behavior as the piezoelectric coefficient as a function of bipolar cycling. Figure 10 illustrates the similarity in the two properties. There are a few possible explanations for the observed increase in  $\epsilon_{33}$  and  $d_{31}$  with cycling: an increase in temperature during cycling and an increase in the net polarization ( $P_{\text{net}}$ ) by improved poling. That is, an increase in temperature could be caused by dielectric losses associated with the ac fields. A small temperature rise would be expected to increase both  $\epsilon_{33}$  and  $d_{31}$ . Alternatively, if imprint has shifted the polarization electric field hysteresis loop far enough along the electric field axis, then the application of a symmetric bipolar field may resemble unipolar operation in a normally poled sample. Therefore,  $P_{\text{net}}$  may increase due to improved poling.

To distinguish the relative importance of these factors, a variety of experiments were conducted. First, it was determined that during cycling a small approximately 2–5 °C temperature rise occurs. Reviewing the results for  $\epsilon_{33}$  versus temperature in Fig. 6, we concluded that this change in temperature during cycling would not provide the necessary increase in the dielectric constant during bipolar cycling. Thus, a rise in temperature can be excluded as a possible mechanism contributing to the increase in  $\epsilon_{33}$  and  $d_{31}$  associated with bipolar drive.

Another possible explanation is the increase in the dielectric constant during cycling may be attributed to a de-aging phenomenon as the concentration or mobility of 180° domain walls increases. During cycling, excitation with an electric field oriented anti-parallel to the poling

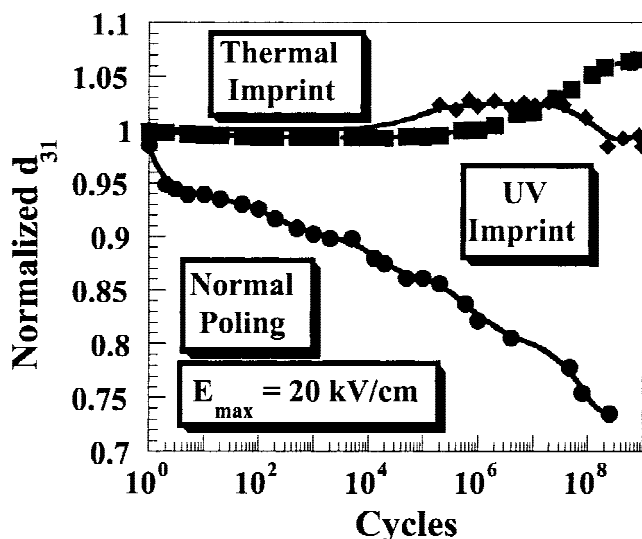


FIG. 9. Effect of imprint on bipolar degradation illustrating the observed trends for each of the poling procedures.

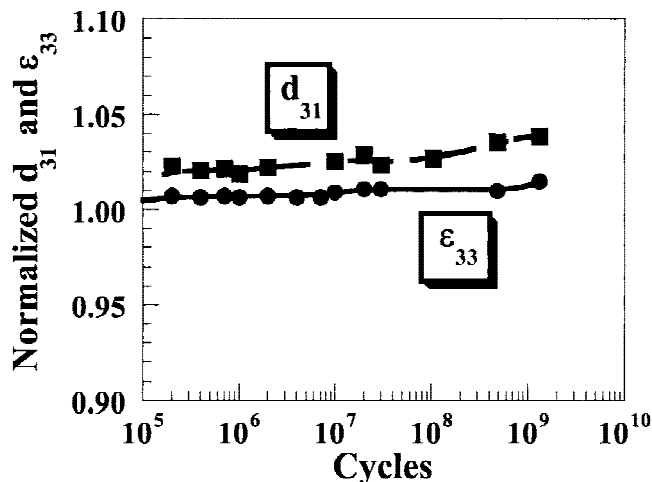


FIG. 10. Changes in  $d_{31}$  and  $\epsilon_{33}$  during bipolar operation (approximately 20 kV/cm) for thermally imprinted 1.0- $\mu\text{m}$ -thick PZT films.

field may destabilize the positions of the walls, so they can be readily perturbed by the measuring field. This would increase the extrinsic contribution to the dielectric constant. The result would be an increased  $\epsilon_{33}$  during bipolar drive.

A polarization–electric field hysteresis loop was taken prior to and after bipolar cycling. From Fig. 11, it can be seen that a small voltage shift increasing the degree of imprint occurs during cycling. Examining the P-E loops for imprinted and normally poled devices (see Fig. 12), it can be seen that a bipolar field of  $\pm 20$  kV/cm traverses the saturation portion of the P-E loop for imprinted devices, similar to a normally poled film driven with a unipolar electric field. Therefore, it is possible that the continuous application of a field oriented parallel to the internal field acts to increase the remanent polarization and hence  $d_{31}$ .

#### IV. CONCLUSIONS

PZT thin films exhibit excellent piezoelectric reliability under unipolar driving fields (approximately 120–400 kV/cm). These films have survived to  $10^9$  cycles with limited changes in the transverse piezoelectric response. The development of a voltage shift (approximately 4–6 kV/cm) in the P-E loop during cycling provides evidence that the  $P_{\text{net}}$  increases during cycling.

However, the  $d_{31}$  coefficient exhibits rapid declines during both aging and bipolar cycling. The mechanism responsible for the large aging rates (6–12%/decade) is depoling of domains due to the influence of internal electric fields generated by both space charges and defect dipole complexes. Similar to aging, field-induced depoling during small amplitude bipolar drive lowers the net polarization, resulting in a rapidly declining  $d_{31}$  coefficient.

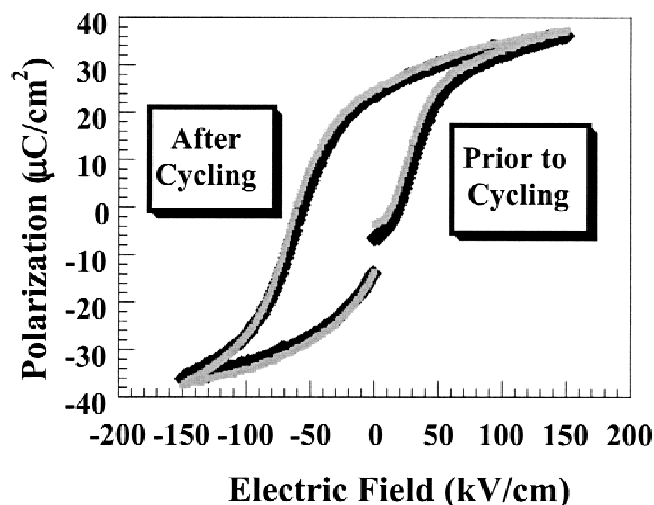


FIG. 11. P-E loops prior to and after bipolar cycling (approximately  $10^8$  cycles).

We also concluded that both UV and thermal imprint can be utilized to improve aging. That is, the relatively modest electric fields that were built into the films via imprint were sufficient to stabilize the polarization and minimize back-switching. Additionally, the development of an internal space charge field during UV illumination limits the charge generated from the direct piezoelectric response and results in diminished piezoelectric coefficients. The subsequent decay of this internal field after exposure increases the piezoelectric coefficient out to  $10^5$ – $10^6$  after poling.

Similar to aging, imprint can improve device performance and lifetime to greater than  $10^9$  cycles under bipolar operating conditions. Again, the space charge field generated during UV imprint plays a critical role in device performance with large increases in the piezoelectric coefficients occurring approximately  $10^3$  seconds after UV poling. During operation, thermally imprinted samples exhibit gradually increasing piezoelectric and dielectric properties during cycling due to increases in the net polarization and increases in either  $180^\circ$  domain wall concentration or mobility, respectively.

#### ACKNOWLEDGMENTS

The authors would like to thank Paul Moses for technical assistance and Defense Advanced Research Projects Agency (DARPA) (contract DABT63-95-C-0053) and National Science Foundation (contract DMR-9502431) for financial assistance. In addition, the authors thank Dr. Clive Randall and Dr. William Warren for helpful technical discussions.

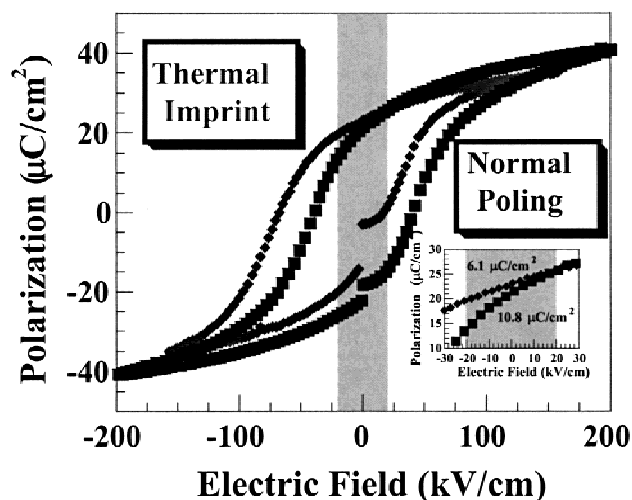


FIG. 12. P-E loop illustrating that a 20-kV/cm (shaded region) bipolar field provides a smaller degree of polarization switching in imprinted devices compared to normal devices.

## REFERENCES

1. D.L. Polla and L.F. Francis, MRS Bull. **21**(7), 59 (1996).
2. T. Tamagawa, D.L. Polla, and C.C. Hsueh, Proc. IEDM, San Francisco, CA, Technical Digest, (IEEE, Piscataway, NJ, 1990), p. 617.
3. A.L. Kholkin, A.K. Tagantsev, E.L. Colla, D.V. Taylor, and N. Setter, Integ. Ferroelectr. **15**, 317 (1997).
4. A.L. Kholkin, E.L. Colla, A.K. Tagantsev, and D.V. Taylor, Appl. Phys. Lett. **68**, 2577 (1996).
5. J.F. Shepard, "The Investigation of Biaxial Stress Effects and the Transverse Piezoelectric ( $d_{31}$ ) Characterization of Lead Zirconate Titanate Thin Films," Ph.D. Thesis, The Pennsylvania State University, University Park, PA (1998).
6. J.F. Shepard, F. Chu, I. Kanno, and S. Trolier-McKinstry, J. Appl. Phys. **85**, 6711 (1999).
7. J.F. Shepard, P.J. Moses, and S. Trolier-McKinstry, Sens. Actuators, **A71**, 133 (1998).
8. J. Lee, R. Ramesh, and V.G. Keramidas, Appl. Phys. Lett. **66**, 1337 (1995).
9. G.E. Pike, W.L. Warren, D. Dimos, B.A. Tuttle, R. Ramesh, J. Lee, V.G. Keramidas, and J.T. Evans, Jr., Appl. Phys. Lett. **66**, 484 (1995).
10. D. Dimos, W.L. Warren, M.B. Sinclair, B.A. Tuttle, and R.W. Schwartz, J. Appl. Phys. **76**, 4305 (1994).
11. W.L. Warren, D. Dimos, G.E. Pike, K. Vanheusden, and R. Ramesh, Appl. Phys. Lett. **67**, 1689 (1995).
12. K.D. Budd, S.K. Dey, and D.A. Payne, Brit. Cer. Proc. **36**, 107 (1985).
13. T. Tuchiya, T. Itoh, G. Sasaki, and T. Suga, J. Ceram. Soc. Japan **104**, 159 (1996).
14. G. Arlt and U. Robels, Integ. Ferroelectr. **3**, 343 (1993).
15. D. Wang, Y. Fotinich, and G.P. Carman, J. Appl. Phys. **83**, 5342 (1998).
16. A. Kholkin, Ferroelectrics **221**, 219 (1999).
17. D. Damjanovic, J. Appl. Phys. **82**, 1788 (1997).
18. B. Jaffe, W.R. Cook, and H. Jaffe, *Piezoelectric Ceramics* (Academic Press, reprinted by R.A.N., Manetta, OH, 1971).
19. M. Kohli, P. Muralt, and N. Setter, Appl. Phys. Lett. **72**, 3217 (1998).
20. X.L. Zhang, Z.X. Chen, L.E. Cross, and W.A. Schulze, J. Mater. Sci. **18**, 968 (1983).
21. A.L. Kholkin and N. Setter, Appl. Phys. Lett. **71**, 2854 (1997).
22. P.S. Brody and F. Crowne, J. Electron. Mater. **4**, 955 (1975).
23. M.E. Lines and A.M. Glass, *Principles and Applications of Ferroelectrics and Related Materials* (Clarendon, Oxford, United Kingdom, 1977).